PROPERTIES OF EPITAXIAL ZnO THIN FILMS FOR GaN AND RELATED APPLICATIONS

H. Shen*, M. Wraback*, J. Pamulapati*, S. Liang**, C. Gorla**, and Y. Lu**

*U.S. Army Research Laboratory, Sensors and Electron Devices Directorate,
AMSRL-SE-EM, 2800 Powder Mill Rd., Adelphi, MD 20783-1197
pshen@arl.mil
**Dept. of Electrical and Computer Engineering, Rutgers University,
Piscataway, NJ 08855-0909

ABSTRACT

In this paper, we present a detailed study of high quality (110) ZnO films, epitaxially grown on R-plane sapphire substrates by metal-organic chemical vapor deposition (MOCVD). The epitaxial relationships are $(11\bar{2}0)$ ZnO//$(01\bar{1}2)$ Al$_2$O$_3$ and $[0001]$ ZnO//$[0\bar{1}11]$ Al$_2$O$_3$ as confirmed by X-ray diffraction (θ-2θ, and ϕ-scan) and high-resolution cross-sectional transmission electron microscopy (HR-TEM). Low temperature photoluminescence (PL) indicates the ZnO thin films are almost strain free. Optical absorption and reflection measurements with linearly polarized light indicate a strong optical anisotropy. The polarization rotation towards the C-axis associated with the optical anisotropy is utilized to demonstrate an optically addressed ultra-fast, ultraviolet light modulator.

INTRODUCTION

High quality zinc oxide (ZnO) films are useful for many applications. One of the more recent applications is the use of ZnO as a substrate for growth of GaN based materials[1-3] since the lattice mismatch between GaN and ZnO is relatively small. Due to a lack of low cost ZnO substrates, high-quality ZnO buffer layers on other substrates are of particular interest. In addition, it is also possible to develop UV lasers and modulators from these ZnO films.[4,5]

The most common technologies used for depositing ZnO films are laser ablation and sputtering.[6] Improvements have been made through triode sputtering and other new deposition techniques. Despite these advancements, there are still some problems associated with sputtering. Metal-organic chemical vapor deposition (MOCVD)[7,8] is an alternative technique for growth that has advantages such as chemical and thermodynamic dependent growth, control at the atomic level, large area deposition, and the possibility of different *in situ* doping processes. While most research has focused on ZnO films grown on (0001) oriented sapphire substrates (i.e. C-plane Al$_2$O$_3$), less research has been done on ZnO grown on other planes. In this paper we report a detailed study of the properties of ZnO grown on $(01\bar{1}2)$ oriented sapphire (R-plane).

SAMPLE GROWTH

The samples used in this study were grown by MOCVD. R-plane sapphire was used as the substrate. The precursors used were DiEthyl Zinc (DEZn − $(C_2H_5)_2Zn$) and O_2. Typical growth conditions are as follows: chamber pressure of 20 to 50 torr; a growth temperature of 250 to 600 °C; and a total carrier gas flow from the top of 5000 to 15000 sccm. The thickness of the sample is 1 μm[9].

STRUCTURAL PROPERTIES

Figure 1 shows the x-ray θ-2θ scans from the sample. From the scan we found that ZnO film has a $(11\bar{2}0)$ orientation. The insert of Figure 2 shows the φ-scan from the $\{21\bar{3}0\}$ family of reflections for ZnO. We found that the angular separation is 180°, the same as predicted by theory for a single crystal. Also shown is the φ-scan from the $\{12\bar{3}5\}$ family of planes from sapphire. The position of the $\{21\bar{3}0\}$ peaks from ZnO and the $\{12\bar{3}5\}$ peaks from Al_2O_3 coincide in the φ-scans. From this we found that the epitaxial relationship for ZnO films grown on R-plane sapphire is:

Figure 1: X-ray 2θ scan, insert: φ-scans of the $\{21\bar{3}0\}$ family of planes.

$$(11\bar{2}0)\,ZnO//(01\bar{1}2)\,Al_2O_3 \text{ and } [0\,0\,0\,1]\,ZnO//[0\,\bar{1}11]\,Al_2O_3.$$

Figure 2 shows a cross-sectional TEM lattice image of the interface between ZnO and R-sapphire. The interface is observed to be atomically sharp and semi-coherent. The 18.3% misfit along the $[1\bar{1}00]$ direction of ZnO is relieved by extra half planes on the sapphire side of the interface. On average, there is one dislocation for every five $(1\bar{1}00)$ planes. The misfit between the two lattices is completely accommodated by misfit dislocations.
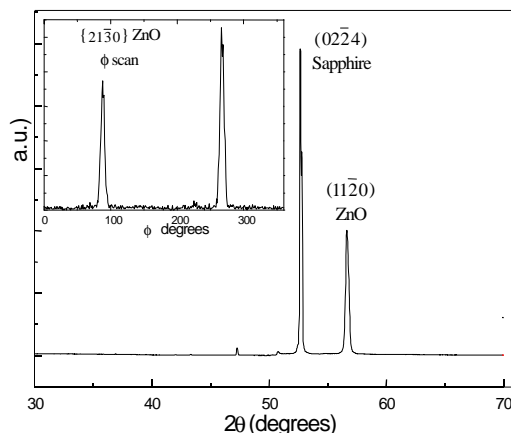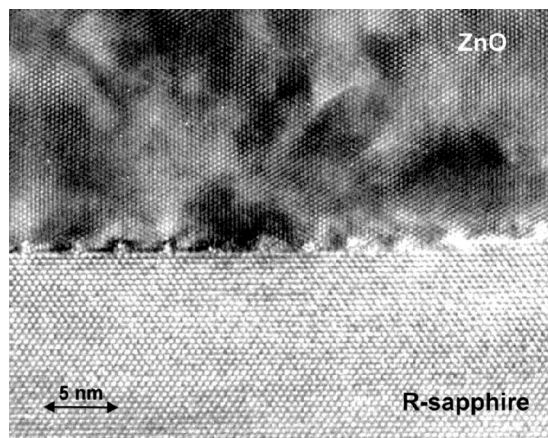

Figure 2: TEM image of the interface between ZnO and R-sapphire. The view is along the c-axis of ZnO .

OPTICAL PROPERTIES

Figure 3(a) shows the room temperature PL spectrum. The feature at 3.28eV is due to band-edge recombination. The broad feature at 2.35eV (green emission) is the recombination of free electrons with holes via interstitial zinc, or via defects at the grain boundaries[10,11]. From Fig. 3(a), the ratio of the integrated intensities of the band-edge emission to the deep level emission (broad band green emission) at room temperature is approximately 3:1. Similar results were observed form ZnO grown by molecular beam epitaxy (MBE)[1].

Figure 3(b) shows the low-temperature PL spectrum collected at 11K. The peak at 3.363eV is from donor-bound exciton (D^{o}X) transition, while the feature at 3.320eV is from the acceptor-bound exciton transition. Note that the position of the D^{o}X is in good agreement with 4K PL results from bulk ZnO[2] indicating that the thin film is almost strain free. The full width at half maximum of this feature is about 6 meV, compared to 3 meV (4.2K) from bulk ZnO and 8.9 meV (4.2K) from ZnO grown on GaN/SiC by MBE, indicating a film of high quality.

We have observed strong optical anisotropy from the ZnO film. Figure 4 shows the transmission T and reflectivity R of the ZnO film measured as a function of photon energy for light polarized parallel and perpendicular to the c-axis of ZnO. Although the shape of the transmission and reflectivity curves are similar for the two polarizations, the curves for $p//c$ are shifted to higher energy by ~20 meV with respect to those for $p^\wedge c$. This phenomenon is primarily related to the anisotropy in absorption associated with the polarization selection rules[12], combined with the separation in energy of the C band from A and B bands. The energy separation of A and B bands is
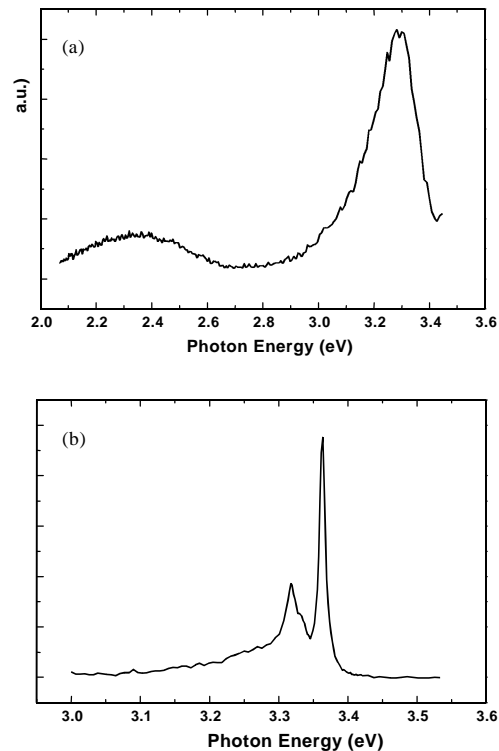

Figure 3: Photoluminescence from ZnO/R-sapphire; (a) room temperature, (b) 10k.
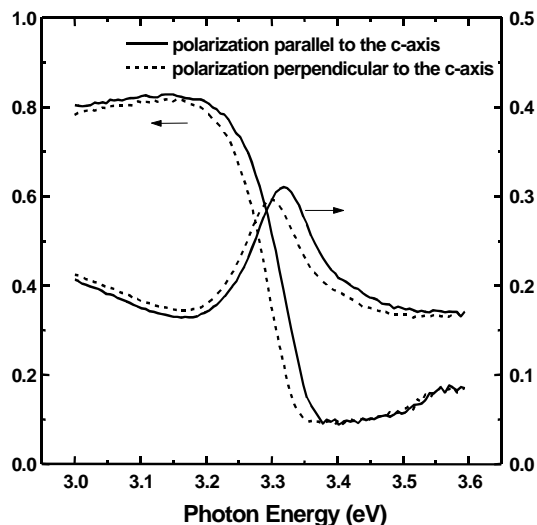

Figure 4: Transmission and Reflectivity of ZnO on R-plane sapphire as a function of photon energy for light polarized parallel (solid lines) and perpendicular (dashed lines) to the c-axis of the ZnO.
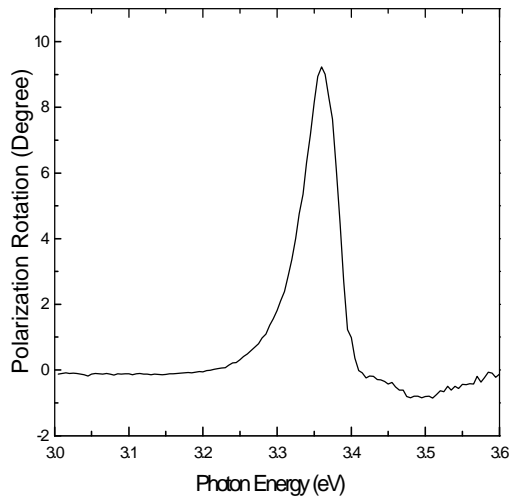
Figure 5: Polarization rotation as a function of photon energy for normal incident light linearly polarized at 45° with respect to the c-axis.

unresolved at room temperature. From a linear fit to the square root singularity, we found that the separation between the A(B) and C bands is about 21 meV, which is significantly smaller than the 40 meV separation measure in bulk ZnO at low temperature (1.6K to 4K). The reason for this is still unclear.

For normal incident light linearly polarized at 45° with respect to the c-axis, we have observed a large polarization rotation toward the c-axis (Figure 5). This rotation is related to the anisotropic absorption with[13]

$$\theta = Tan^{-1} [(T_{//} / T_{\perp})^{1/2}] - 45°$$

where $T_{//}$ and $T_{\perp}$ are the transmission for $p//c$ and $p \wedge c$, respectively. A maximum rotation of 10° occurs at 3.335 eV. This rotation was used to demonstrate a high-contrast, high-speed ultraviolet light modulator.
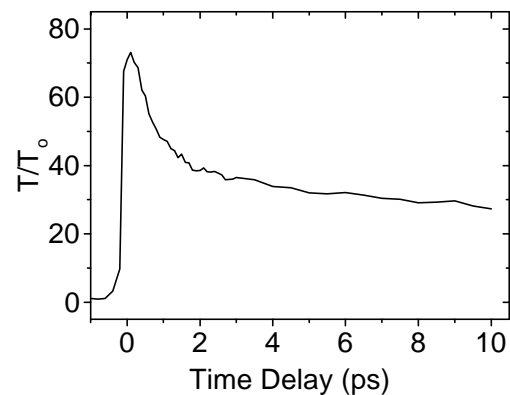
OPTICAL MODULATOR

We use ultraviolet pulses with a center wavelength corresponding to the static rotation maximum to test the modulator. The polarization of the prove pulse was oriented at 45° with respect to the c-axis of the ZnO modulator. Another ultraviolet pulse (pump pulse) is used to control the intensity of the transmitted probe pulse. The transmission of the probe at the photon energy corresponding to the maximum static rotation was monitored as a function of the delay time between the pump and probe pulses. A phase compensator and polarizer placed after the modulator were oriented for minimum transmission of the probe in the absence of the pump[14].

Figure 6: Normalized probe transmission as a function of time delay between the pump and probe pulses.

Figure 6 shows the normalized probe transmission T/T_o through the crossed polarizer as a function of time delay. T_o is the transmission in the absence of the pump. At negative time delays, for which the probe precedes the pump, $T/T_o=1$, as expected. As the pump and probe pulses become temporally coincident in the modulator, a sharp, pulse-width limited rise in probe transmission is observed at time delay $\tau=0^+$ which reaches a maximum more than 70 times

greater than its value for negative time delays. This peak value in the normalized transmission is defined as the contrast ratio for the device. The pump-induced transmission possesses an initial decay time of 0.75 ps, followed by a slower decay to a quasi-equilibrium value within 100 ps (not shown). Subsequent return to equilibrium occurs on a nanosecond time scale. The full width at half maximum of the modulation curve is less than 3 ps.

CONCLUSION

We have studied the structure and optical properties of high quality epitaxial ($11\bar{2}0$) ZnO films on ($01\bar{1}2$) sapphire substrates. The epitaxial relationship has been determined. TEM results indicate that the interface is semi-coherent. A sharp, excitonic, band-edge PL peak obtained at 11K indicates a strain free film that exhibits excellent quality. We have also observed a strong optical anisotropy that is utilized in a normal incidence, high-contrast, ultraviolet light modulator.

REFEREENCES

1. M. A. L. Johnson, S. Fujita, W. H. Rowland, Jr., W. C. Huges, J. W. Cook, Jr., and J. F. Schetzina, Journal of Electronic Materials, **25**, 855 (1996).
2. F. Hamdani, A. Botchkarev, W. Kim, H. Moorkoc, M. Yeadon, J. M. Gibson, S.-C. Y. Tsen, D. J. Smith, D. C. Reynolds, D. C. Look, K. Evans, C. W. Mitchel and P. Hemenger, Appl. Phys. Lett., **70**, 467 (1997).
3. F. Hamdani, M. Yeadon, D. J. Smith, H. Tang, W. Kim, A. Salvador, A. E. Botchkarev, J. M. Gibsor, A. Y. Polyakov, M. Skowronski, and H. Morkoc, J. Appl. Phys. **83**, 983 (1998).
4. P. Zu, Z. K. Tang, G. K. L. Wong, M. Kawasaki, A. Ohtomo, H. Koinuma, and Y. Segawa, Solid State Commun., **103**, 459 (1997).
5. D. M. Bagnall, Y. F. Chen, Z. Zhu, T. Yao, S. Koyama, M. Y. Shen, and T. Goto, Appl. Phys. Lett, **70**, 2230 (1997).
6. V. Srikant, V. Sergo, and D.R. Clarke, J. Am. Cer. Soc. **78**, 1931 (1995).
7. P. Roth, and D. F. Williams, J. Appl. Phys. **52**, 6685 (1981)
8. B. Cockayne, and P. J. Wright, J. Crystal Growth, **68**, 223 (1984).
9. C. R. Gorla, N. W. Emanetoglu, S. Liang, W. E. Mayo, Y. Lu, M. Wraback, and H. Shen, to be published in J. Applied Physics
10. S. Takata, T. Minami and H. Nanto, Jpn. J. Appl. Phys. **20**, 1759 (1981).
11. S. Tanaka, K. Takahashi, T. Sekiguchi, K. Sumino, and J. Tanaka, J. Appl. Phys. **77**, 4021 (1995).
12. W.Y. Liang and A.D. Yoffe, Physical Review Letters, **20**, 59 (1968).
13. H. Shen, M. Wraback, J. Pamulapati, M. Dutta, P.G. Newman, A. Ballato, and Y. Lu, Appl. Phys. Letts. 62, 2908 (1993).
14. M. Wraback, H. Shen, S. Liang, C.R. Gorla, and Y. Lu, to be published in Appl. Phys. Letts.